Nondestructive Testing and Evaluation

ISSN: 1058-9759 (Print) 1477-2671 (Online) Journal homepage: www.tandfonline.com/journals/gnte20

Investigations of strength and quality of clinched joints using digital image correlation

Mohanna Eshtayeh & Meftah Hrairi

To cite this article: Mohanna Eshtayeh & Meftah Hrairi (2025) Investigations of strength and quality of clinched joints using digital image correlation, Nondestructive Testing and Evaluation, 40:9, 4088-4113, DOI: 10.1080/10589759.2024.2416002

To link to this article: https://doi.org/10.1080/10589759.2024.2416002

NONDESTRUCTIVE TESTING AND EVALUATION
2025, VOL. 40, NO. 9, 4088–4113
https://doi.org/10.1080/10589759.2024.2416002

Taylor & Francis
Taylor & Francis Group

Investigations of strength and quality of clinched joints using digital image correlation

Mohanna Eshtayeh[a,b] and Meftah Hrairi[a]

[a]Department of Mechanical and Aerospace Engineering, International Islamic University Malaysia, Kuala Lumpur, Malaysia; [b]Research and Development Department, Aeon Metal Industries, Amman, Jordan

ABSTRACT

This study examines the impact of processing conditions on joint strength and the effectiveness of digital image correlation (DIC) in detecting failure points in clinched joints. Mechanical tests, including single-lap shear and pull-out tests, were conducted using DIC to evaluate joint quality in various clinched configurations. The results showed frequent failures at the neck rejoin in clinched joints between mild steel and aluminum sheets, particularly when thinner sheets were positioned on the punch side and softer materials on the die side. DIC effectively identified defects and failure locations, offering insights into material combinations, sheet positioning, and failure modes. Although DIC was useful in detecting defects in both elastic and destructive regions, its ability to distinguish specific defect types from strain contour maps was limited. The study highlights the need for further research to extend DIC's application to other mechanical joining systems and advocates for its proactive use in refining designs and manufacturing processes.

ARTICLE HISTORY
Received 12 September 2023
Accepted 4 October 2024

KEYWORDS
Aluminium; clinching; digital image correlation; joint failure; joint quality; steel

1. Introduction

Mechanical joining technology plays a vital role in product development by providing various advantages and disadvantages of joining methods. Clinching, a quick mechanical fastening technique, is particularly suitable for connecting dissimilar, coated and hard-to-weld lightweight sheet materials [1,2]. The use of clinching has gained popularity in industrial sectors such as aerospace and automotive, where reducing product weight and joining challenging materials are critical. During the formation of clinching joints, two phenomena are observed: reduction in sheet thickness at the neck location and the generation of tensile cracks in the lower sheets [3,4]. Clinching can be classified based on joint geometry and the configuration of the die type, such as extendable or conventional fixed-die [5,6]. Tensile–shear tests have shown comparable joint strength for both types, with the extendable die requiring lower forming force. The use of an extensible die has also resulted in a larger interlock length and higher strength values when tested using the peeling technique [7].

The primary factors that exert a significant influence on the strength of clinch joints encompass the interlock length, bottom thickness and the presence of joint defects. In

CONTACT Meftah Hrairi meftah@iium.edu.my

this context, Digital Image Correlation (DIC) plays a crucial role in identifying the initiation points of failure during the loading of the specimen. In essence, it serves as a valuable tool for pinpointing the onset of failure or the detection of defects within the joints prior to the occurrence of plastic deformation, specifically before reaching the yield point. The investigation of clinched joints using DIC finds particular value in several industries and applications. Specifically, the automotive industry benefits significantly from DIC analysis of clinched joints, where these joints are extensively used in vehicle body assembly for joining components such as sheet metal panels and structural members. Additionally, aerospace and transportation sectors rely on clinched joints for lightweight construction and assembly of aircraft and trains, making DIC analysis vital for ensuring the integrity and durability of these critical structures. Furthermore, the manufacturing industry, including sectors such as appliances, electronics, shipbuilding and bridges, also leverages clinched joints for diverse applications, making DIC an invaluable tool for quality control, process optimisation and failure analysis in these fields.

Formability and material strength in addition to the joint geometry affect the strength and the quality of the clinched joint, while an optimisation of the clinching joints reflects different relations between factors. The key factors affecting the neck and the bottom thickness include, for example, the die height, die diameter, punch diameter and punch corner radius. Additionally, punch diameter with draft angles is crucial for the bottom thickness and interlock length, while increasing the bottom or neck thickness reduces interlock. Further research is needed to optimise the relationship of these parameters relative to the spring back, tensile strength and separation force evaluation in clinching joint damage. Moreover, the DIC can be used as a non-destructive, non-contact method to determine the quality of the joints and to detect the defects related to the main parameters affecting the strength of the clinching joint [7]. By analysing strain distribution during clinching, DIC guides process adjustments, validates simulations and identifies failure modes. These insights enhance our understanding and enable advancements in clinched joint technology.

DIC has been utilised in various studies involving joining processes by measuring strain fields at the joint, which can be correlated with the damaging behaviour, eg in-situ shear-lap tests in self-piercing riveted joints [8] and in bolted joints [9]. It has been used to measure full-field displacements and analyse the stress states in these joining methods [10]. Comparative studies between spot resistance welding and clinched joints have employed DIC to determine in-plane strain distribution [11]. Innovative methods have been introduced for joining aluminium alloy 5052 sheets using hybrid resistance spot clinching, where heat generated by current is utilised. DIC was used to evaluate the distortion behaviour of the weld joints during testing. Compared with the stiffness of traditional joints, the higher stiffness of the resistance spot clinching joint generated a higher tensile stress component in the periphery of the fusion zone during testing [12]. In a comprehensive investigation, transfer learning techniques were employed to identify cracks on concrete walls, complemented by structural health monitoring utilising the DIC technique to track crack propagation over time. The combination of these two methodologies can offer an effective approach to assess and establish the efficiency of structures in categorising and localising diverse forms of cracks, spalls and other flaws within concrete buildings in real-world environments. This integrated approach holds

the potential to automate the damage detection process, streamlining and enhancing the overall structural integrity assessment [13]. An innovative addition to the steel construction realm comes in the form of cold-formed steel (CFS) T-Stub connections. These connections, utilising a combination of self-drilling screws and Howick rivet connectors (HRC), showcase exceptional structural performance in the building industry. The integration of clinching joining methods presents an avenue for exploration. By combining this novel method with traditional steel structure joining techniques, a thorough examination is conducted using the advanced Digital Image Correlation (DIC) technique to inspect and analyse the efficacy of these joining methods [14,15].

The key advantages of using DIC method for investigating the quality of clinched joints compared to traditional methods lie in its ability to provide high spatial resolution, full-field surface strain measurements without contact, enabling comprehensive analysis of deformation and stress distribution and quantitative data. Additionally, DIC is non-invasive and suitable for in-situ testing, facilitating real-time monitoring and analysis of joint quality during manufacturing processes, thus enhancing efficiency and quality control in clinched joint production. While DIC offers several advantages, it also has some limitations when applied to the study of clinched joints. Proper surface preparation is crucial for accurate DIC measurements, and achieving an optimal speckle pattern can be challenging. Lighting conditions impact image quality, and DIC assumes small deformations within the field of view. Detecting out-of-plane movements, handling varying material thickness and addressing environmental factors are essential. Additionally, DIC involves intensive computation, assumes linear elastic behaviour and requires expertise for meaningful postprocessing and interpretation of results. Diligent planning and calibration can enhance measurement reliability.

DIC offers several advantages for investigating the quality of clinched joints, it is essential to consider factors like cost, equipment requirements, expertise in setting up and using DIC systems and it can be helpful in the model analyses and the validation of FEM. The choice between DIC and traditional methods may depend on the specific needs of the application and the available resources [16,17]. Implementing Digital Image Correlation (DIC) for clinched joint assessment involves varying costs and complexities, influenced by equipment, software and expertise. Expenses include high-quality cameras, lighting and specialised software, with setup and calibration adding to complexity. Despite these challenges, DIC offers significant benefits, providing detailed data on deformation and strain for a thorough joint analysis. The decision to use DIC depends on project needs, weighing the detailed analysis benefits against costs and complexities for improved understanding and reliability in assessing clinched joints [17].

Digital Image Correlation (DIC) offers an economical and expeditious testing method. This research introduces a pioneering application of the DIC technique, employing it as a Non-Destructive Testing (NDT) approach for evaluating clinching joints. The fundamental concept involves subjecting the joint to the anticipated maximum load it would experience under real operational conditions (ie the design load) while capturing two images: one prior to loading and one after. The subsequent analysis of these two images using DIC software enables the identification of surface or subsurface defects, primarily due to localised strain concentrations ‘strain map’ in and around the defected areas. It is essential to emphasise that the design load remains significantly below the structure’s failure load (yield

point), incorporating a safety margin (ie ensuring the material remains within the elastic region).

So far, the DIC technique has been widely applied in the manufacturing area, including cutting, welding, forming, additive manufacturing, etc. due to its high performance. To the authors' knowledge, DIC technology was not utilised in the field of clinching joint defects and failures. However, the potential for investigating its significant impact on joint quality and defect detection could be explored in future research endeavours. Indeed, DIC could be used in the analysis of the clinched joint, including uniaxial tensile measurement of clinched joints for the study of constitutive behaviour and analysis of crack strain field of clinched joint for studying fatigue and fracture behaviour.

The primary goal of this work is to assess the impact of processing conditions on joint strength, specifically in clinching, and to explore the application of Digital Image Correlation as a non-destructive testing tool for detecting failure points in clinched joints. The study seeks to contribute to the existing body of knowledge by integrating DIC into the assessment of clinched joints, providing valuable insights into joint quality and failure modes. The unique contribution of the paper lies in proposing DIC as a cost-effective and efficient method for evaluating the quality of clinched joints. The integration of DIC into the assessment of joint strength, failure modes and defect detection adds a novel dimension to the existing literature on mechanical joining technologies. The paper underscores the versatility of DIC, not only in the field of clinching but also in other applications, demonstrating its efficacy in diverse engineering scenarios.

2. Digital image correlation technique

Digital image correlation is an optical experimental technique to perform full field strain measurements using a series of sequential images of a surface taken by a single camera for 2D measurements or by two or more cameras for 3D measurements. In essence, DIC measurements are made by comparing two digital images of the material surface acquired at different loading stages, one image that corresponds to the undeformed state (reference image), and the other that corresponds to a partial or to the final loading stage (deformed image). Calibration is necessary to initialise the spatial correlation processes of DIC. To start with the correlation process, the reference and the deformed images are first subdivided into small square regions containing several pixels called subsets. Then, the DIC algorithm uses a correlation function to identify matching regions of subsets in both the reference and the deformed states. The displacement field is then computed. The density of the displacement measurements is controlled by the step size (eg with a step size of 1, displacements are computed at every pixel). Subsequently, the strain field is obtained by derivation on displacement gradients. To perform this process efficiently, the surface of the object must have a high-contrast granular morphology. Therefore, the samples usually must be prepared beforehand by first painting their surfaces, for example with a thin layer of white paint, and then applying over them a random pattern of black dots (speckle pattern).

In the context of evaluating clinched joints, the fundamental concept involves subjecting the joint to the anticipated maximum load it would experience under real operational conditions (ie the design load) while capturing two images: one prior to loading and one after. The subsequent analysis of these two images using DIC software

enables the identification of surface or subsurface defects, primarily due to localised strain concentrations 'strain map' in and around the defected areas. It is essential to emphasise that the design load remains significantly below the structure's failure load (yield point), incorporating a safety margin (ie ensuring the material remains within the elastic region). Consequently, this inspection method is unequivocally classified as a non-destructive technique.

Implementing Digital Image Correlation (DIC) for clinched joint assessment involves varying costs and complexities, influenced by equipment, software and expertise. Expenses include high-quality cameras, lighting and specialised software, with setup and calibration adding to complexity. Despite these challenges, DIC offers significant benefits, providing detailed data on deformation and strain for a thorough joint analysis. The decision to use DIC depends on project needs, weighing the detailed analysis benefits against costs and complexities for improved understanding and reliability in assessing clinched joints [17].

Anticipating future developments and innovations in the use of Digital Image Correlation (DIC) for analysing clinched joints, there are several possibilities: (1) Integration of DIC with other advanced characterisation techniques for advanced material characterisation, automation and artificial intelligence may play a significant role in the analysis of DIC data measuring displacements and assess joint integrity. (2) Real-time DIC monitoring during the clinching process could become more practical, allowing for immediate feedback and quality control. (3) Advancements in imaging technology and software algorithms may lead to higher resolution DIC systems, enhancing accuracy in strain and displacement measurements. (4) DIC data may be integrated more seamlessly with finite element analysis and simulation tools, improving the predictive capabilities of joint behaviour and performance. (5) Different industries, such as automotive, aerospace and construction, may develop specialised DIC techniques and practices to address their unique requirements for clinched joint analysis. These future developments could lead to more effective and widespread use of DIC technology in studying clinched joints, ultimately enhancing the reliability and performance of these joints in various applications.

3. Materials and methods

3.1. Materials

In this study, a range of metal sheets were carefully chosen to encompass various material types and conditions, with the aim of investigating the potential impact on clinched joints. The sheet materials used for this study were mild steel SPCC as defined in JIS G 3141 standard [18], galvanised steel Z180 and aluminium alloys AA1100 and AA5052. The ASTM E08 standard guided the performance of uniaxial tensile test. An Instron 3367 universal testing machine equipped with a load cell at a constant speed of 2 mm/min was used to perform the tests. Table 1 lists the principal mechanical properties of sheets that were tested.

Figure 1 shows the clinching tools, extendable die (consisted of three sliding sectors), punch and blank holder. The used clinching machine and the set of the extensible die

Table 1. Mechanical properties of mild steel SPCC, galvanised steel Z180 and aluminium alloys AA1100 and AA5052.

Material designation	Thickness (mm)	Elastic modulus (GPa)	Yield strength (MPa)	Tensile strength (MPa)	Elongation at fracture (%)
SPCC	0.8; 1.0	197	270	328	36.4
Z180	1.0; 1.2	205	174.5	252	28.3
AA1100	1.0	68.9	105	125	20
AA5052	1.5	60.8	154.9	219.5	16.6

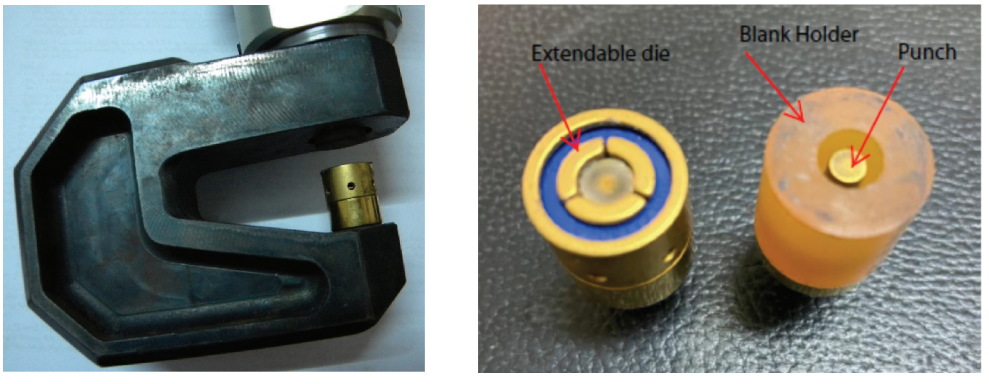

(a) Clinching machine with extensible die

(b) Clinching tools: extendable die, blank holder, and punch.

Figure 1. Clinching tools, extensible die, punch and blank-holder.

clinching punch and die with plank holder are shown below whereas, clinching tools (punch and die) are made from high strength steel.

3.2. Specimen configuration and preparation

To assess the strength of various clinching joint configurations, a series of tests were performed on different types of materials. All tensile–shear tests were performed in accordance with ISO 12,996: 2013 guidelines for single-lap joint specimens [19]. Testing of the clinched joints' load-carrying capacity was performed on 30 × 100 mm test samples. Figure 2a shows the geometry of the test specimen used in these tests. Since limited research has been done to investigate the mechanical behaviour of multiple clinched joints in configurations and the way they affect each other in terms of maximum strength [20,21], different clinched joints, based on alternative arrangement of clinched points, were produced. Indeed, the specimens included single, double and quadruple clinched points using mild steel plates, galvanised sheets and aluminium alloy. The different configurations of the clinched points are depicted in Figure 2.

A BTM Pneumo-hydraulic Clinch Unit type ULG7–10 system, depicted in Figure 1, was used as the clinching machine. All clinching joints were formed under a consistent press force of 28 kN. Mild steel and aluminium sheets, varying in thickness from 0.5 mm to 1.25 mm, were subjected to a 4.6 mm punch diameter, while sheets with a thickness of 1.5 mm utilised a slightly reduced punch diameter

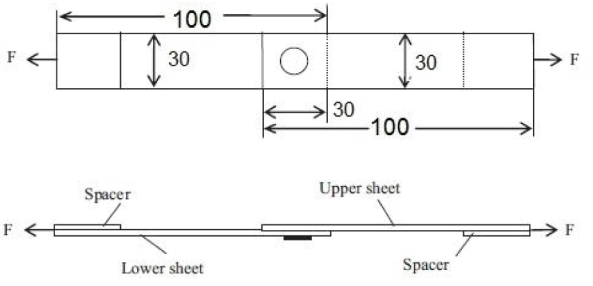

(a) Dimensions (in mm) of the test specimen

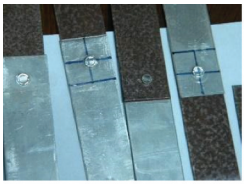

(b)Single clinch

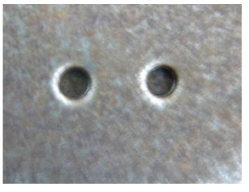

(c) Double clinch (vertical)

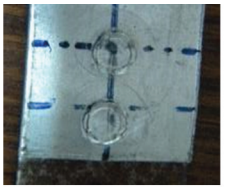

(d) Double clinch (horizontal)

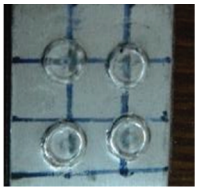

(e) Four clinched

Figure 2. Specimen geometry and samples configuration of the clinch points.

of 3.8 mm. The die diameter for all clinching joints remained constant at 4.6 mm. The clinching machine, seamlessly connected to the necessary pressurised source, played a pivotal role in these precision operations. Alignment of the two sheets was achieved by inserting the C claw of the clinching machine, creating the clinched joint precisely at the desired location. Subsequent to the preparation of clinched specimens featuring a random black–white speckle pattern, experiments were conducted following the specified procedure. Throughout the experiments, all specimens underwent loading via displacement control, maintaining a constant speed rate of 1 mm/min. The specimens were securely mounted onto the tensile machine and the testing machine underwent calibration, setting displacement and load values to zero. The CCD camera was then positioned to ensure the clinched joint occupied the central position on the screen. Ensuring the camera's perpendicular alignment to the specimen's surface, its focus was adjusted, and an initial reference image was recorded. Subsequently, the camera was configured to capture images at 10-s intervals. The loading of the specimen commenced simultaneously with the initiation of image capture by the camera. The loading process persisted until the specimen reached load failure, at which point the test was promptly terminated. This systematic approach ensured comprehensive data collection on the behaviour of clinched joints under controlled conditions.

To facilitate the description of the clinched joints made with the extendable die using different sheets, the designations used to describe the different types of joints, the specimen combinations, nomenclature and the number of specimens for each clinching configuration are shown in Table 2.

Table 2. Designation and nomenclature of the different manufactured joints.

Nomenclature	Upper sheet	Lower sheet)	Type of joint	No of specimens
SCSTA	SPCC (t = 1.0mm)	AA1100	Single point clinched (Figure 5a)	15 (8 with corroded surfaces)
SCAST	AA1100	SPCC (t = 1.0mm)	Single point clinched (Figure 5a)	2
SCALST	AA1100	SPCC (t = 0.8 mm)	Single point clinched	5
SCGIAL	Z180	AA1100	Single point clinched	5
SCSTAL	SPCC (t = *1.5mm*)	AA5052	Single point clinched	4
SCSTAL-H	SPCC (t = *1.5mm*)	AA5052	Single point clinched-adhesive	3
SCSTA -H	SPCC (t = 1.0mm)	AA1100	Single point clinched-adhesive	4
SCALST -H	AA1100	SPCC (t = 0.8 mm)	Single point clinched-adhesive	10 (5 with 0.15 mm and 5 with 0.35 mm adhesive thickness)
DCSTA	SPCC (t = 1.0mm)	AA1100	Double point clinched (Figures 5b, c)	3
DCGIAL	Z180	AA1100	double point clinched	4
DCSTA H	SPCC (t = 1.0mm)	AA1100	Double point clinched-adhesive	3
FCSTA	SPCC (t = 1.0mm)	AA1100	Four points clinched (Figure 5d)	2
$SCSTAL_{pullout}$	SPCC (t = 0.8 mm)	AA1100	Single point clinched	5

Tensile loading was applied to the specimens using a universal testing machine (INSTRON-3367), with the loading direction perpendicular to the clinched point, as shown in Figure 3.

During the clinching process, the material experiences rapid spreading, leading to interlocking when using the extensible die clinching method. The clinched joints were formed using a clinching machine with equal stroke extension, which depended on the thickness of the bottom sheet. A fixed forming force was applied to achieve the clinched joint for different material combinations. Various clinched joint configurations were investigated in this study, as depicted in Figure 4.

3.3. Hybrid clinched joint

The same procedure used for forming clinched joints was applied to create clinch-bonded hybrid joints. In this study, a two-component acrylic steel epoxy resin and hardener were used as the adhesive (4-min steel epoxy manufactured by Silock Technical Inc) [22]. The selected steel epoxy exhibited high performance and remained constant throughout the study. The strength of the joint depended on the installation process, which involved several steps. The mechanical properties of the adhesive were as follows: Young's modulus of 2 GPa and Poisson's ratio of 0.30. To ensure better penetration between the epoxy layer and the plates, a rough cleaned surface was necessary. The epoxy adhesive was mixed and applied over the required overlap area, with a resin-to-hardener ratio of 1:1. Clinching was performed after a curing time of 2–3 min. The epoxy adhesive was allowed to

Table 3. Tensile–shear test results of clinched joints (mild steel and AA1100, 1.0 mm thickness).

Specimens	Maximum load (N)	Energy absorption (J)*
SCSTA 1	1859.46	2.46
SCSTA 2	1832.44	1.95
SCSTA 3	1705.90	2.07
SCSTA 4	1765.62	2.14
SCSTA 5	1887.42	2.01
SCSTA 6	1952.44	2.58
SCSTA 7	1915.25	2.54
SCSTA 8	1859.97	1.77
SCSTA 9	1891.67	1.05
SCSTA 10	1847.97	1.68
SCSTA 11	1813.84	2.29
SCSTA 12	1890.66	1.17
SCSTA 13	1853.95	1.65
SCSTA 14	1896.19	1.14
SCSTA 15	1979.36	1.06

*The area under the displacement–load curve.

Figure 3. Universal shear tension machine with clinching sample.

cure for approximately 24 h before conducting testing using a universal tensile–shear testing machine. The curing period aimed to enhance the joint's strength by allowing the adhesive layer to fully set. Figure 5 illustrates the clinch hybrid bonded joints with DIC patterns.

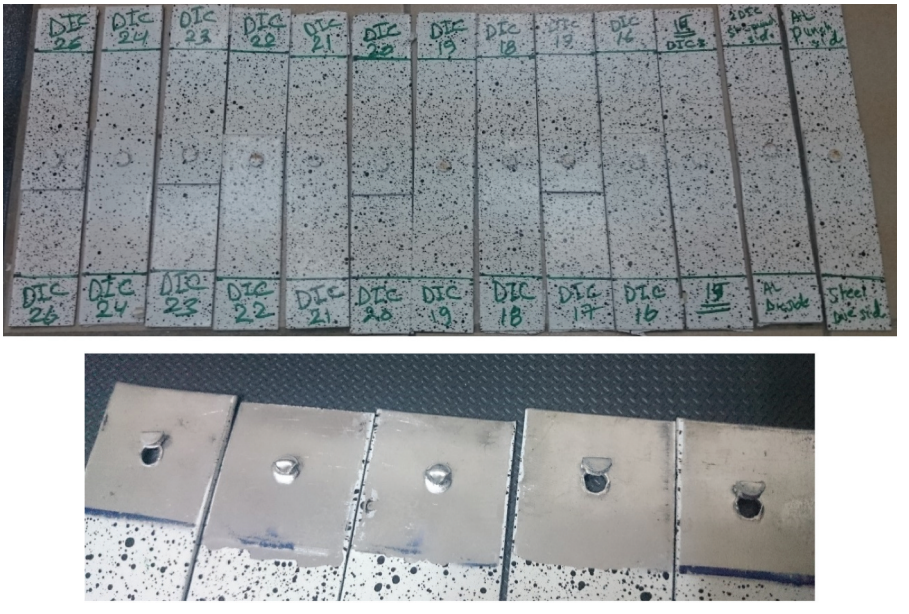

(a) Single point clinched joint with failure mode

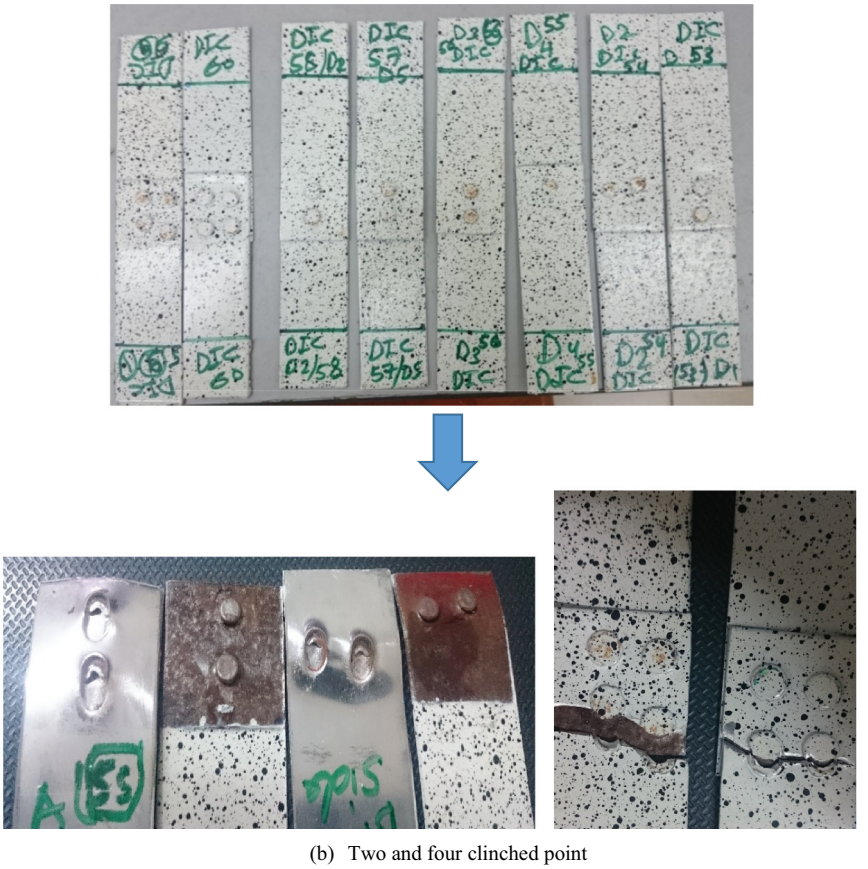

(b) Two and four clinched point

Figure 4. Clinching joints with different configurations with white and black pattern and failure modes.

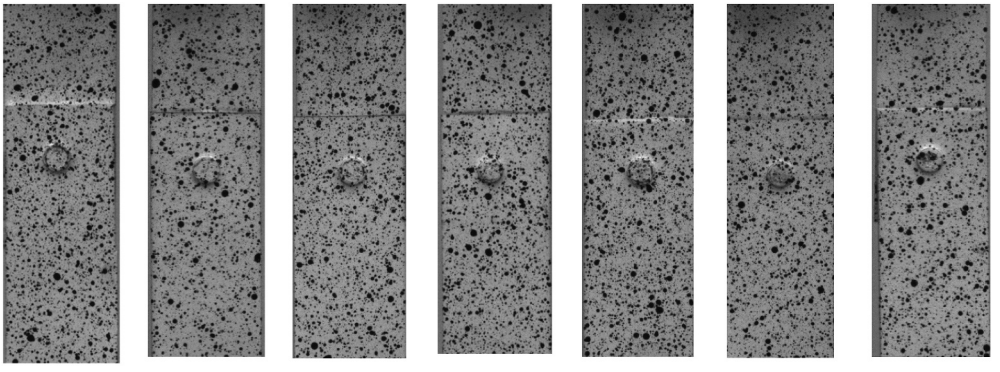

Figure 5. Hybrid clinching joints with different configuration with white and black pattern.

3.4. Digital image correlation sample preparation

To prepare the samples for digital image correlation analysis, the following steps were taken. The specimen was initially cleaned through sandblasting, and its surface finish was examined. If the surface was too smooth, coarse sandpaper was used to roughen it, providing grooves for the paint to adhere to. Good paint adhesion was crucial as the specimen would undergo strain during testing. A final cleaning was performed to remove any residue from the sanding process.

A thin coat of white paint was applied to the region of interest on the specimen. It was important to ensure the white paint layer's thickness was controlled, as excessive thickness could lead to poor elastic qualities and surface cracks at low displacements. Subsequently, a random black pattern was sprayed onto the specimen using black spray paint. It was essential to maintain a uniform amount of black paint during each

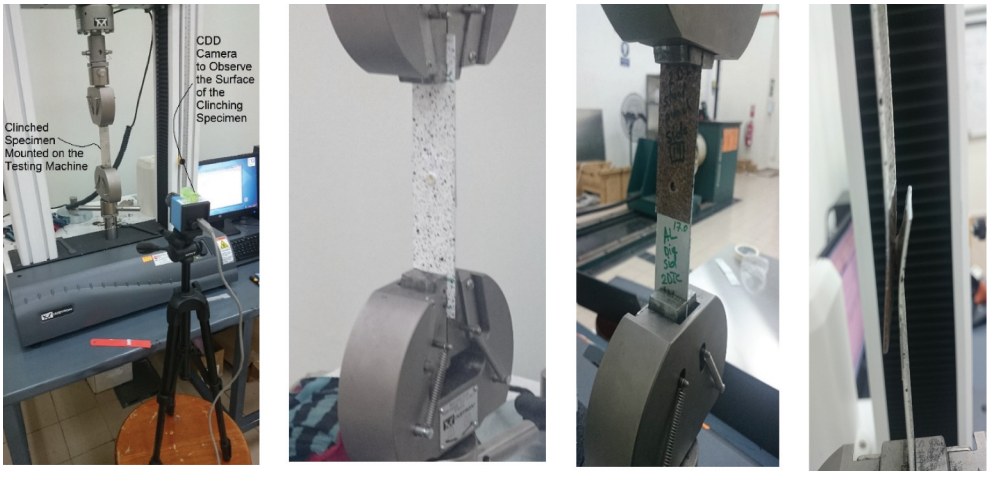

(a) Equipments of the experiment

(b) Front face of the specimen with the white black pattern

(c) Rear side of the specimen

(d) side view of the sample during failure mode.

Figure 6. Experimental set-up.

coating, ensuring consistent delivery. Additionally, a typical random speckle pattern was applied. Samples with the white and black patterns are depicted in Figure 5.

3.5. Experimental procedure

After preparing the clinched specimens with the random black and white speckle patterns, the experiments were conducted as follows. All specimens were loaded using a displacement control system at a constant speed of 1 mm/minute. The specimen was securely mounted in the fixture of the universal tensile machine using sample grips. The testing machine was calibrated, setting the displacement and load to zero, with the calibration process integrated into a computer system.

A CCD camera was mounted and focused, positioned to ensure that the clinching joint was approximately projected to the centre of the camera's view. The camera's alignment was adjusted to ensure it was perpendicular to the specimen's surface. The initial reference image (first image) was captured by the camera without any load. The camera was set to capture images at a rate of one frame per second.

The universal machine was then started, loading the specimen while simultaneously triggering the CCD camera to capture images. Loading of the specimen continued until the failure point, at which the testing machine was stopped. The CCD camera was manually stopped at the same time. The experimental setup is illustrated in Figure 6.

Digital image correlation (DIC) using Vic-2d software and a CCD camera (The imaging source DMK41BU02) was utilised to detect the starting point of clinched joint failure. The captured images had a resolution of 1280×960 pixels, with one capture per second.

This investigation primarily depends on the plastic deformation region, which occurs beyond the yield strength of the respective materials. For instance, the yield strength for the mild steel plate was measured as 270 MPa, while the aluminium A1100 alloy exhibited a yield strength of 105 MPa. Hence, the stress value corresponding to 0.66 of the yield strength (ie 1.5 factor of safety) was around 70 MPa (105 MPa × 0.66) for aluminium and 178 MPa (270 MPa × 0.66) for mild steel. The load value for the clinched specimens can be calculated with reference to the Force/Area, by considering a specimen area of 30 mm^2 (30 mm (width) × 1 mm (thickness)):

- For Mild steel 1.0 mm sheet thickness: Force/Aera = 178 MPa resulting of a force of 5.3 kN.

- For Aluminium 1.0 mm sheet thickness: Force/Aera = 70 MPa resulting of a force of 2.1 kN.

It is crucial to emphasise that these stress values are applicable when the specimen remains undamaged, without the introduction of any joints. It should be recognised that the anticipated failure load for clinched joints is expected to be lower than these values. Indeed, the load-deformation characteristics of a specific sample, featuring a clinched joint, were meticulously observed. The graph (Figure 8) highlights the 2.1 kN load level, accompanied by its corresponding deformation value, with the loading process continuing until the specimen reaches fracture. Notably, the 2.1 kN load falls within the elastic region of deformation, signifying a non-destructive phase in the material's response to stress.

This stress level ensured that the material remained within the elastic region, avoiding permanent deformation after load release. The initial image was taken before loading the

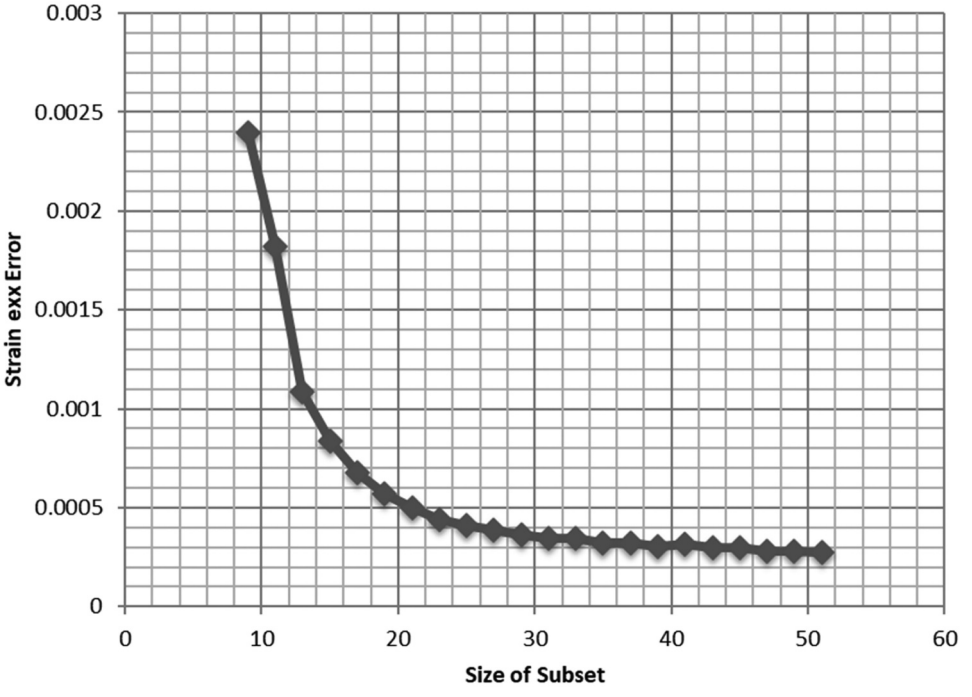

Figure 7. Error estimation diagram with subset size variation along the x-axis translation.

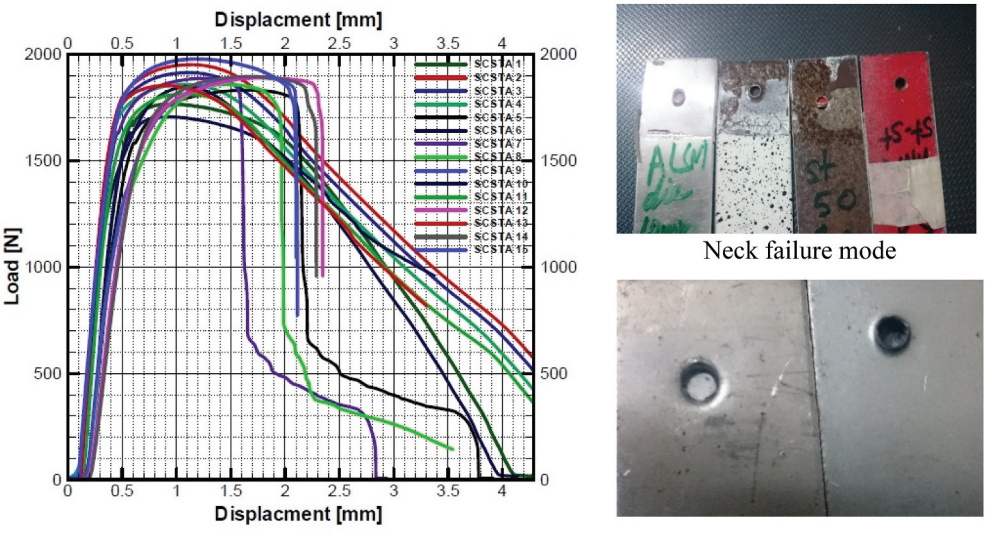

Figure 8. Displacement versus load curves for clinched joint single lap with specimens' view after failure (neck failure mode).

specimen, and an image was captured when the stress level was below the yield strength (elastic region) for NDT conditions. A safety factor of approximately 1.5 was assumed for the plate's stress level in engineering applications.

Several parameters in the DIC analysis, such as step size, subset and strain window size, were set before running the correlation to achieve accurate results. Subset size (number of pixels) controlled the displacement tracking between the initial and deformed image areas, while the step size controlled the distance between points. To assess subset size's impact on correlation results and determine the suitable size for this investigation, various correlations were conducted on the same area using different subset sizes. In-plane rigid-body translation experiments estimated strain error magnitudes for these subsets [23]. Images of a specimen were taken at different positions and correlated, with the strain value indicating error. Subset sizes were systematically adjusted, ranging from 9 to 51 pixels, with a step size of half the subset size. The strain error values for each size are shown in Figure 7. The error decreases rapidly with larger subsets, stabilising beyond 30 pixels. An excessively large size could overly smooth results, making 29 pixels (with a 14-pixel step) ideal for subsequent correlations in this investigation.

Digital Image Correlation (DIC) has strengths and limitations in clinched joint research. Challenges include surface preparation, 2D nature and gradient limitations. Calibration is vital. Despite these, DIC is valuable for material deformation studies due to its advantages in full-field measurements and detailed strain data. Diligent planning and calibration can enhance measurement reliability.

4. Results and discussion

A servo-hydraulic universal shear–tensile testing machine with hydraulic grips was employed to test the clinched joint specimens. The specimen length between the grips was approximately 170 mm, and spacers with sheet thickness were used to centralise the load during experiments. All clinched joints were tested at a constant displacement rate of 1 mm/minute. The testing machine's integrated software continuously recorded data, including force–displacement curves, during each test.

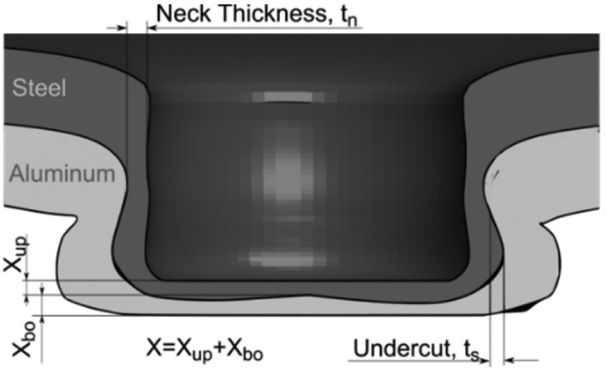

Figure 9. Geometrical parameters of the clinching process bottom thickness "X", neck thickness "tn", and undercut (interlock length) "ts".

The tested materials were AA1100 aluminium alloy and mild steel, both with a thickness of 1.0 mm. In this set of specimens, the mild steel was positioned at the punch side. Table 3 presents the tensile–shear test results for the clinched joints, and Figure 8 illustrates the displacement–load curves for the 15 tested specimens. The results show that the average maximum load across the 15 specimens was 1863.47 N, with an average energy absorption of 1.83 J. Additional specimens of the same materials were tested, with the aluminium alloy AA1100 located at the punch side and the mild steel sheet at the die side.

In addition, specimen No. 8 to 15 have less energy absorption due to the corroded mild steel used in these samples. While the strength of the joint was found to lie

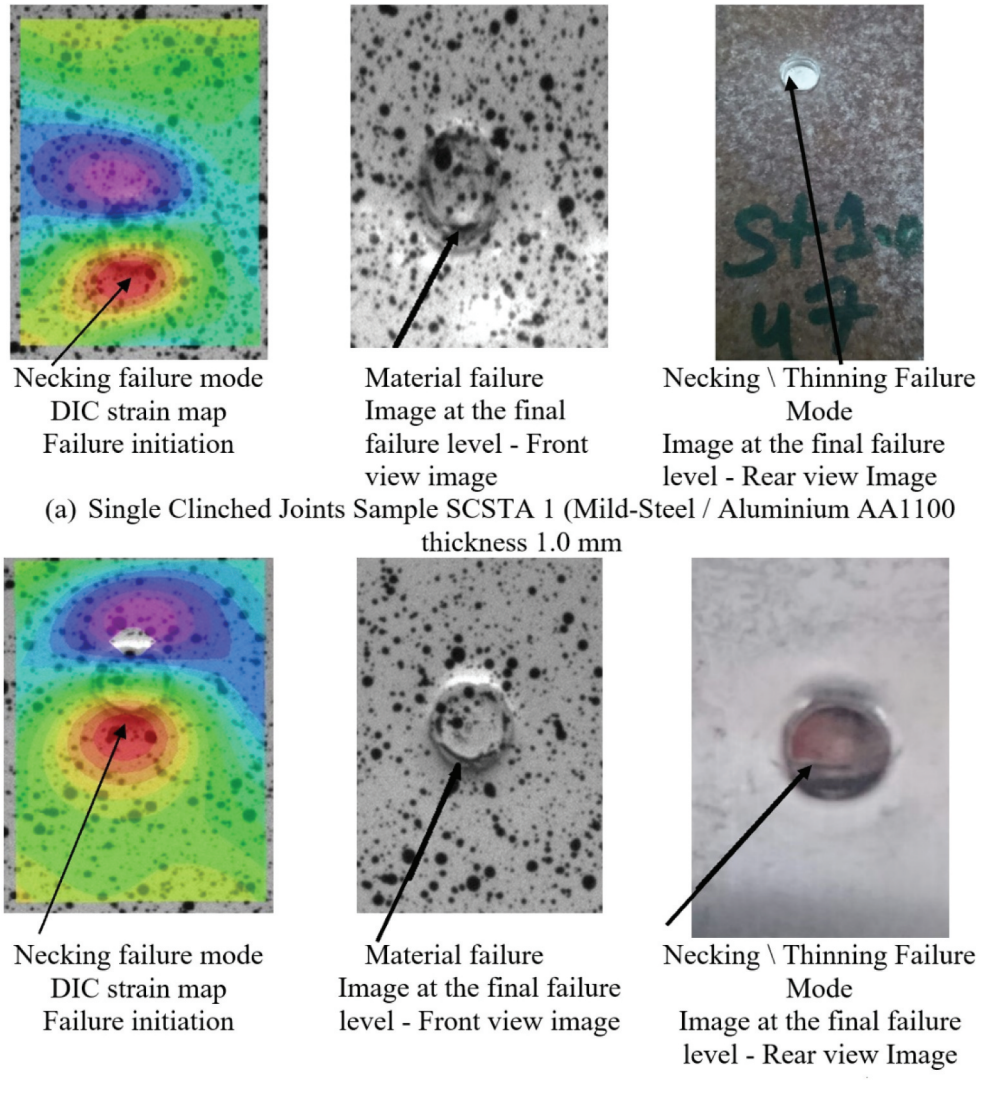

Figure 10. Clinched joints with DIC strain contour map plots (single clinched point with interface failure).

approximately in the same range. It seems that corrosion resulting in a sudden fracture may create a defect during the clinching process.

As illustrated in Figure 9, the main parameters affecting the clinching joint behaviour include the interlock length (undercut) denoted by ts, bottom thickness represented by x and neck thickness indicated as tn. These parameters intricately influence the strength of the joints. Notably, significant relationships exist among these parameters due to the complicated nature of joint formation and the material flow dynamics during the creative process. The largest interlock induces a reduction in neck thickness. The failure of clinching joints under loading during tensile tests is exacerbated by the thinning of the neck area of the upper sheet. The increase of the interlock length thereby increases the overall strength of the clinched joint causing a reduction in the thickness after formation at the neck area. This necessitates a more extensive exploration through experimental and optimisation methodologies to attain a comprehensive understanding of the interrelations among these joint parameters. This investigative endeavour is underpinned by the integration of advanced scientific techniques, specifically finite elements, and the digital image correlation technique. The synthesis of these methodologies aims to expose the nuanced dependencies between interlock length, bottom thickness and neck thickness, contributing to a profound comprehension and optimisation of clinching joint strength.

The purpose of utilising DIC in this study was to identify the starting point of clinch joint failure during tensile testing. The universal shear–tensile machine and CCD camera operated simultaneously, with the load data obtained from the machines used to determine the load value corresponding to each captured image. A total of around 70 clinched joint samples with rectangular overlap shapes were tested, encompassing different configurations of clinching joints. Black and white patterns were applied to most of the samples to collect additional information using the DIC setup, including the integration of tensile–shear tests with DIC techniques.

Figure 10 depicts the selected tension test specimens' configurations and their corresponding DIC strain contour map plots for single clinched joints with their failure modes. The results demonstrate that failure initiation in the elastic region below the yield strength occurs at the bottom of the clinched joint for samples SCSTA1 and SCSTA2, clearly indicated by the high strain concentration around the joint in the DIC contour map. The final stage of clinched joint failure also occurs at the same location, as observed in the front view photo of the final stage. On the backside of the images, the failure type is classified as an interface failure, where the fracture of the upper sheet at the interlocking part is caused by thinning of the neck thickness. The results indicate a good interlock length between the two sheets, evaluated based on the interlocking length (ts) and neck thickness (tn) of the upper sheet.

In practical applications, the tensile–shear stress is the primary load borne by joints, and it was specifically considered in our study. Figure 11 presents the DIC strain contour maps of specimens SCSTA3, SCSTA4 and SCSTA11. These maps reveal that the defect initiates at the upper circumference point of the clinched joint. Moreover, the front view image obtained from the CCD camera during the final stage of loading depicts a change in the shape of the clinched joint, transitioning from a circular shape to an oval shape (deformed-back side view). This change in shape signifies the initiation of failure associated with the joint section's shape.

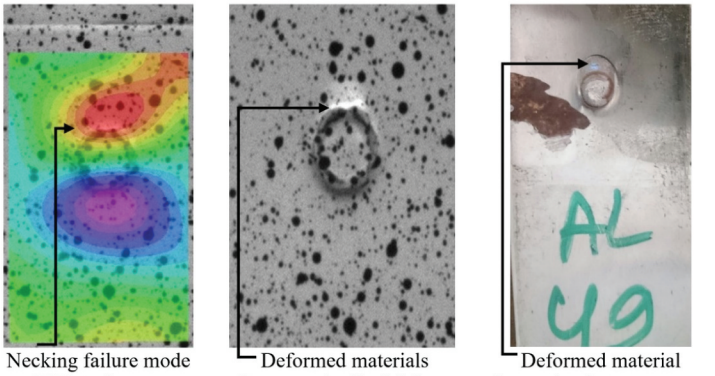

(a) Single Clinched Joints Sample SCSTA 3 (Mild-Steel / Aluminium AA1100 thickness 1.0 mm

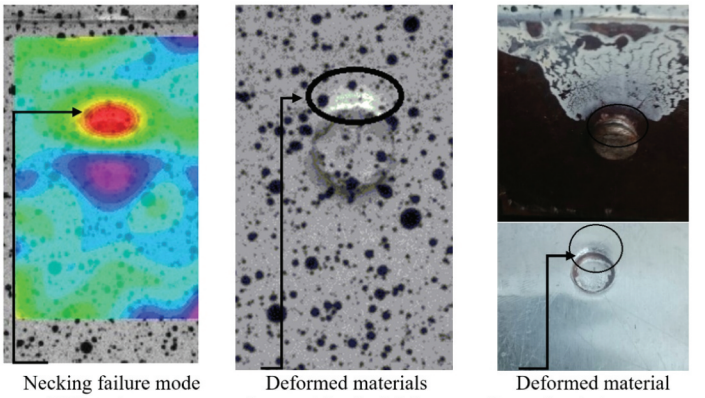

(b) Single Clinched Joints Sample SCSTA 4 (Mild-Steel / Aluminium AA1100 thickness 1.0 mm

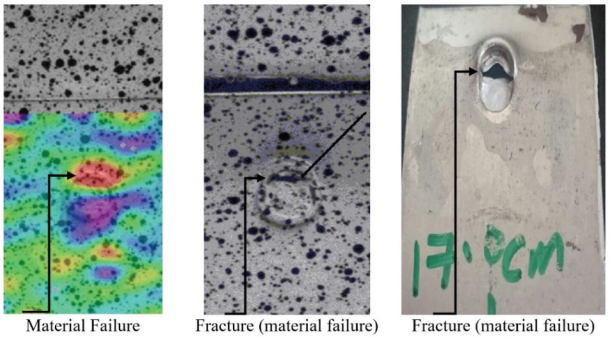

(c) Single Clinched Joints Sample SCSTA 11 (Mild-Steel / Aluminium AA1100 thickness 1.0 mm

Figure 11. Clinched joints with DIC strain contour map plots (single clinched point with combined fracture mode).

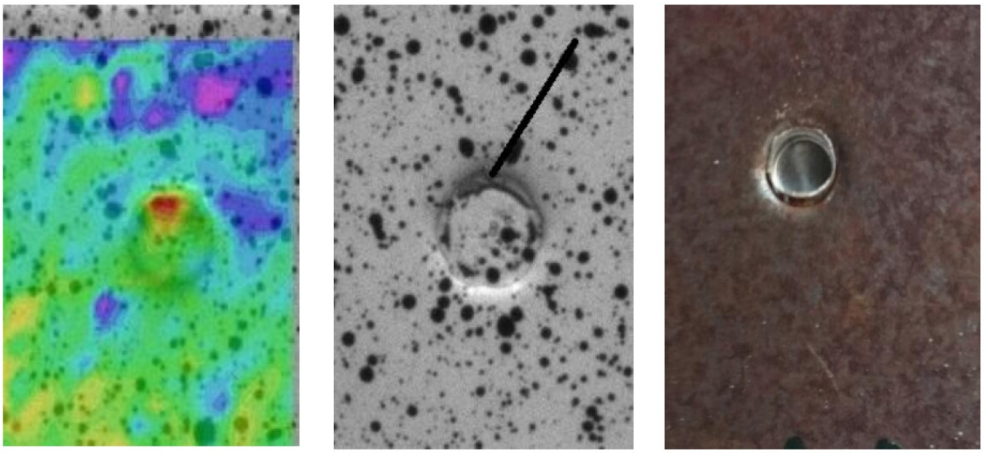

Figure 12. Clinched joints with DIC strain contour map plots (single clinched point with thinning at the neck failure mode).

As previously mentioned, the presence of a small neck thickness can lead to fracture in the upper sheet at the thinnest point of the neck. Based on the obtained results, it can be concluded that the failure mode in this case is the separation between the upper and lower sheets due to insufficient interlocking between them, exacerbated by the material joints at the bottom of the joint. Furthermore, when observing the specimens from another perspective after completing the final stage of the test, it becomes evident that the ultimate failure location is indeed at the bottom, consistent with the findings from the DIC contour map.

In the case of sample SCSTA11, the rear-view image reveals a stronger clinched joint compared to the other samples, with failure occurring only after the material itself fractures completely. This can be considered as a combined fracture mode (Figure 11).

As previously mentioned, the main failure modes of clinching include unbuttoning, neck fracture, or a combination of both mechanisms. The location of the sheets was observed to be a crucial factor influencing the strength of the clinched joint. Specimen SCAST1, where the aluminium is positioned at the punch side, exhibited a lower joint strength (1002 N) compared to clinched joints with mild steel at the punch side (average value 1863 N). This indicates that the joint can be considered weak. The lower strength of the clinched joint can be attributed to the limited interlocking length between the two sheets and the material locking at the bottom area of the joint.

Figure 12 displays the DIC strain contour map, illustrating that the crack initiates at the top section of the clinched aluminium sheet. Furthermore, both the front and back view images obtained during the final stage of the test confirm these results. To analyse the type of failure mode that occurred, it can be attributed to material thinning at the neck of the aluminium sheet, leading to the failure of the clinching joint.

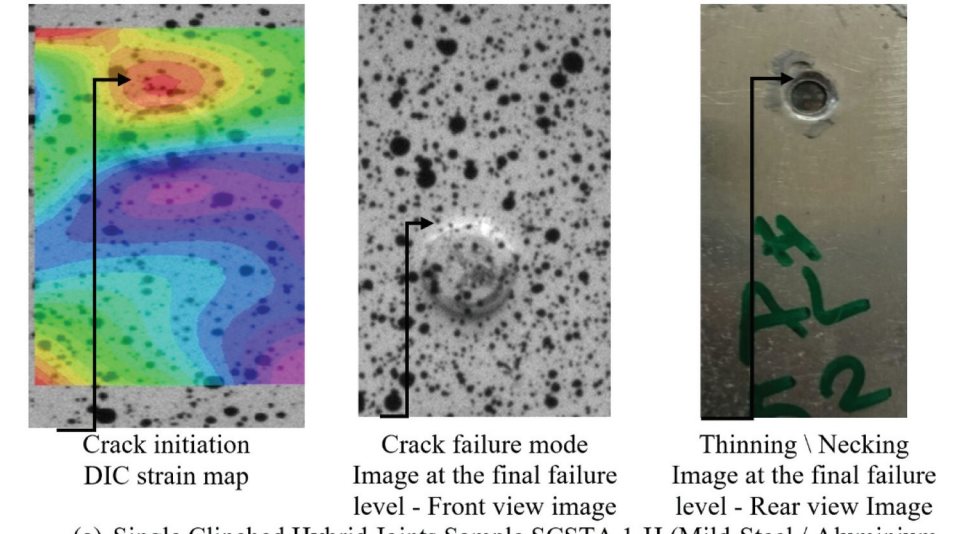

Figure 13. Clinched joints with DIC strain contour map plots (single clinched point with thinning at the neck failure mode).

In most joint variants, the shear test results exhibited high repeatability. This can be attributed to meticulous specimen preparation and consistent assembly under the same test conditions. Specimens SCSTA-H1 and SCSTA-H3 were single lap clinched hybrid joints, with mild steel positioned at the punch side. The load–displacement curve results indicate that the average joint strength was 1907 N, surpassing the strength of conventional clinched joints (1800 N).

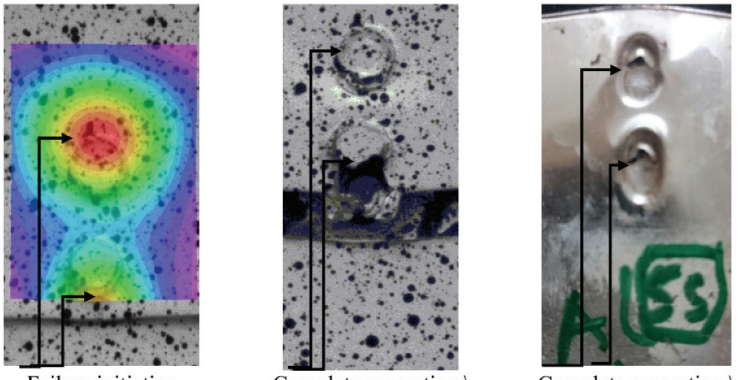

Failure initiation DIC strain map | Complete separation \ rupture Image at the final failure level - Front view image | Complete separation \ rupture Image at the final failure level - Rear view Image

(a) Double Clinched Joints Sample DCSTA 1 (Mild-Steel / Aluminium AA1100 thickness 1.0 mm)

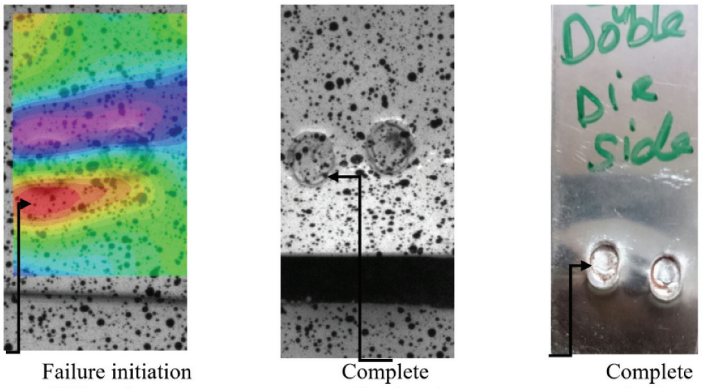

Failure initiation DIC strain map | Complete separation \ rupture Image at the final failure level - Front view image | Complete separation \ rupture Image at the final failure level - Rear view Image

(b) Double Clinched Joints Sample DCSTA 2 (Mild-Steel / Aluminium AA1100 thickness 1.0 mm) (Double clinched point)

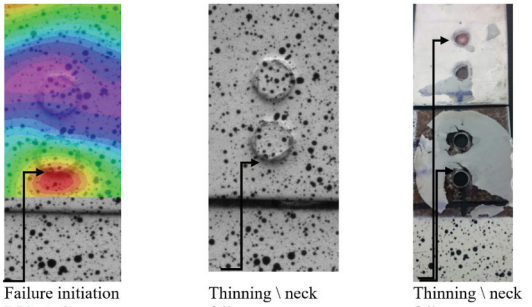

Failure initiation DIC strain map | Thinning \ neck failure Image at the final failure level - Front view image | Thinning \ neck failure Image at the final failure level - Rear view Image

(c) Double Clinched Hybrid Joints Sample DCSTA 3-H (Mild-Steel / Aluminium AA1100 thickness 1.0 mm)

Figure 14. Clinched joints with DIC strain contour map plots (single hybrid clinched point pull-out failure).

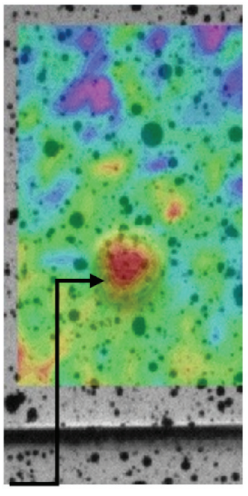

Failure initiation
DIC strain map

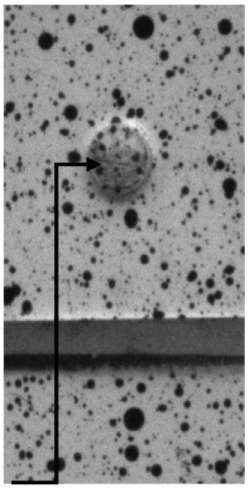

Image at the final failure level - Front view image

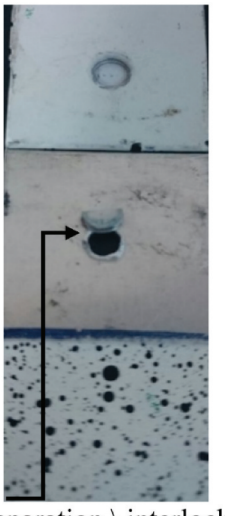

Separation \ interlock failure
Image at the final failure level - Rear view Image

(a) Single Clinched Joints Sample SCALST 2 (Mild-Steel 0.8 mm / Aluminium AA1100 thickness 1.0 mm)

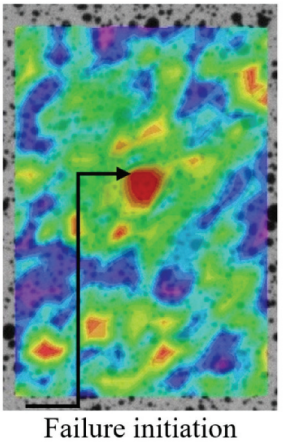

Failure initiation
DIC strain map

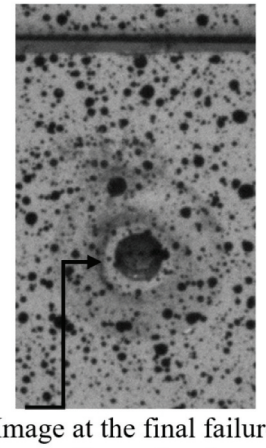

Image at the final failure level - Front view image

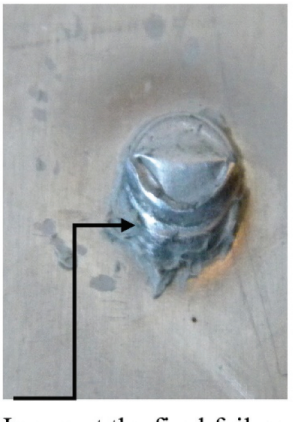

Image at the final failure level - Rear view Image

(b) Single Clinched Hybrid Joints Sample SCALST 6 H (Mild-Steel 0.8 mm / Aluminium AA1100 thickness 1.0 mm)

Figure 15. Clinched joints with DIC strain contour map plots (single clinched point and hybrid clinched points).

The DIC strain contour map reveals that crack initiation occurred at the top portion of the aluminium sheet. Similarly, the back view image confirms these results at the final stage of the test. However, the front view image of the final stage does not provide clear information, as shown in Figure 13. Failure can be defined as the complete separation or rupture of the specimens into two parts. The results suggest

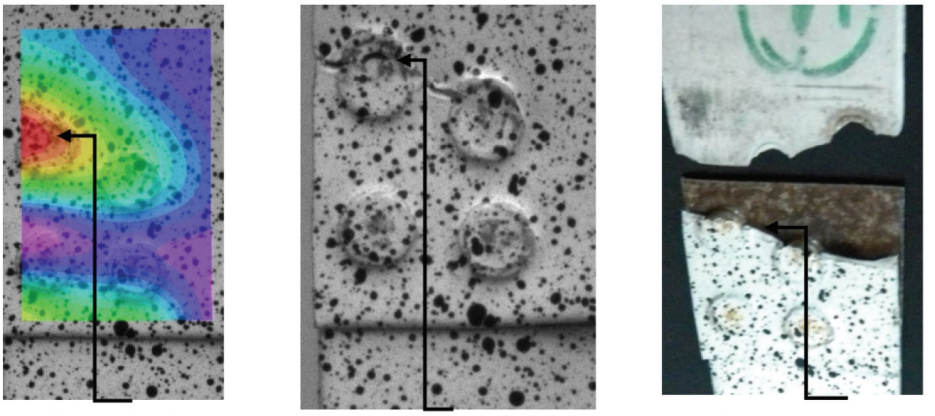

Failure initiation
DIC strain map

Material failure \ final stage
Image at the final failure level - Front view image

Material failure
Image at the final failure level - Rear view Image

(a) Four Clinched Joints Sample FCSTA 1 (Mild-Steel 1.0 mm / Aluminium AA1100 thickness 1.0 mm)

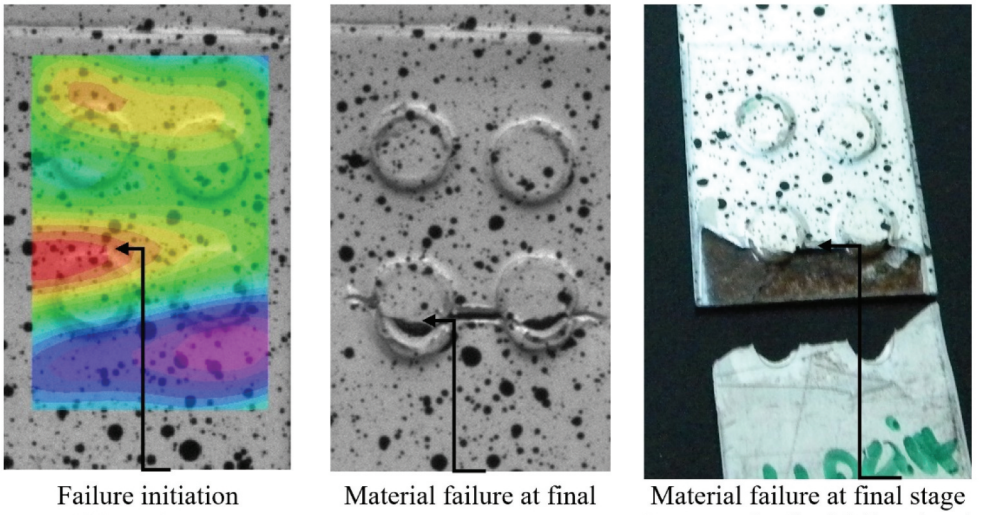

Failure initiation
DIC strain map

Material failure at final stage
Image at the final failure level - Front view image

Material failure at final stage
Image at the final failure level - Rear view Image

(b) Four Clinched Joints Sample FCSTA 2 (Mild-Steel 1.0 mm / Aluminium AA1100 thickness 1.0 mm)

Figure 16. Clinched joints with DIC strain contour map plots (four clinched points).

that the failure mode can be attributed to the thinning of the upper aluminium sheet until material rupture.

In certain cases, the tensile–shear specimens experienced pull-out failure mode, indicating that the punch force did not adequately reach the required force for joining the upper and lower sheets together.

Clinched joints with a large interlock, achieved using an extendable die, exhibit higher stiffness, especially when multiple clinched points are employed. The tensile–shear test results for vertically and horizontally double clinched joints indicate greater strength (2870 N) compared to single clinched joints (1826 N).

To detect defects in the elastic region of dissimilar materials, specifically mild steel (1.0 mm) and AA1100 (1.0 mm), the DIC technique was applied to the vertical and horizontal (aligned with the tensile force direction) clinched joints. Specimens DCSTA1, DCSTA2 and DCSTA3-H, as shown in Figure 14, were analysed. The strain map reveals that the initial failure occurred at the first clinched point (top clinched point), which experienced a higher load. The front and rear views of the specimens display the joint failures, aligning with the DIC results.

However, in the case of specimen DCSTA3-H, a double hybrid horizontal clinched joint with two points, the final stage image demonstrates necking failures at both clinched points under high-stress conditions.

The strength of clinched joints is found to be influenced by the material of the upper sheet. In the case of using mild steel with a thickness of 0.8 mm and aluminium sheets AA1100 with a thickness of 1.0 mm, the tensile test results indicate that achieving a satisfactory clinching joint requires using aluminium sheets with greater thickness (1.0 mm) on the punch side.

The DIC strain contour map, as shown in Figure 15, for samples SCALST2 and SCALST6-H (single clinched and adhesive joint using mild steel 0.8 mm and aluminium alloy AA1100 with 1.0 mm thickness) reveals concentrated strain at the centre of the clinched point. This concentrated strain suggests that this area serves as the initial starting point of joint failure, primarily due to neck thinning or other defects subjected to the applied load. The front view image from the camera does not provide clear indications in the clinching bulge, while the rear view of the aluminium alloy sheets shows a mixed failure mode at the clinched joint, characterised by separation between the upper and lower sheets resulting from interlock failure. In most cases, when the stronger sheet is positioned in front of the camera during testing, especially when an additional material such as adhesive is present, the front view image does not reveal any signs of failure.

Specimens FCSTA1 and FCSTA2 (Mild Steel with AA1100/1.0 mm thickness) featuring a four-point clinched joint exhibit higher strength (3207 N) attributed to the increased number of clinched points. The correlation results indicate a red area in the strain contour map, specifically located at the top left clinch point. In line with the study's focus on the elastic region, the starting failure point aligns with the concentrated strain indicated by the red area in the DIC strain contour map. The front view image confirms that the failure originates from the same point depicted in the DIC strain contour map. The failure mode of the quadruple clinched joint can be categorised into normal mode, observed during the tensile–shear test and abnormal mode. In this case, the failure mode involves material rupture, with the crack propagating through the clinched point. Figure 16 showcases the DIC counter map illustrating the failure mode at the final stage of the tensile test. Additionally, the final observations reveal that some of the clinched points remain intact, connecting the two sheets, while the other two clinched points are completely disconnected.

5. Conclusion

This study delved into the potential of Digital Image Correlation (DIC) for pinpointing the initial failure point within the elastic region before yielding in clinched joints. Various clinched sample configurations underwent experimental tensile–shear tests in tandem with the DIC technique. The analysis of load–displacement curves determined the mechanical properties of the joints, while the investigation examined the observed failure modes. Key discoveries from this research include:

- **Material Combinations and Clinched Points**: Combining similar and dissimilar metal sheets (AA1100 with mild steel) yielded robust-clinched joints using the extendable clinching die system. Multiple clinched points enhanced the strength, but excessive adhesive weakened the clinched joint, causing complete separation between the upper and the lower sheets.
- **Effectiveness with Dissimilar Thickness**: Dissimilar metal sheets with different thicknesses had been effectively joined with the extendable clinching die, with thin sheets on the punch side (upper sheet).
- **Critical Role of Sheet Positioning**: Positioning mild steel on the punch side in the tensile–shear clinched joint resulted in more strength of the clinched joint and more load-bearing joints.
- **Factors Influencing Failure Modes**: The type of failure mode depended on interlock length, neck thickness and bottom thickness of the joint. Larger interlock lengths may cause thinning in the neck area, reducing the clinched joint strength.
- **DIC Capability**: DIC effectively identified failures and defects in clinching joints within both elastic (non-destructive) and destructive regions. However, depending exclusively on DIC results may not observe specific joint defect types.
- **Limitations of DIC Strain Contour Map**: The DIC strain contour map alone cannot determine the failure mode. Further investigations are needed to evaluate its suitability for different mechanical joining systems.

Despite the promising findings of this study, one should highlight the need for subsequent research to explore DIC's applicability in identifying failure modes across various mechanical joining systems beyond clinching. Employing DIC to identify joint defects prior to failure offers engineers valuable insights. These findings empower engineers to proactively refine clinched joint designs and manufacturing processes, resulting in enhanced robustness and efficiency across a broad spectrum of engineering applications.

Disclosure statement

No potential conflict of interest was reported by the author(s).

References

[1] Eshtayeh M, Hrairi M. Recent and future development of the application of finite element analysis in clinching process. Int J Adv Manuf Technol. 2016;84(9–12):2589–2608. doi: 10.1007/s00170-015-7781-z

[2] Eshtayeh MM, Hrairi M, Mohiuddin AKM. Clinching process for joining dissimilar materials: state of the art. Int J Adv Manuf Technol. 2015;82(1–4):179–195. doi: 10.1007/s00170-015-7363-0

[3] Lee C-J, Kim J-Y, Lee S-K, et al. Parametric study on mechanical clinching process for joining aluminum alloy and high-strength steel sheets. J Mech Sci Technol. 2010;24(1):123–126. doi: 10.1007/s12206-009-1118-5

[4] Eshtayeh M, Hrairi M. Multi objective optimization of clinching joints quality using grey-based Taguchi method. Int J Adv Manuf Technol. 2016;87(1–4):233–249. doi: 10.1007/s00170-016-8471-1

[5] Atia MKS, Jain MK. A novel approach to hot dieless clinching process for high strength AA7075-T6 sheets. Proc IMechE, Part C: J Mech Eng Sci. 2020;234(19):3809–3825. doi: 10.1177/0954406220917406

[6] Tenorio MB, Lajarin SF, Gipiela ML, et al. The influence of tool geometry and process parameters on joined sheets by clinching. J Braz Soc Mech Sci Eng. 2019;41(2):67. doi: 10.1007/s40430-018-1539-0

[7] Lambiase F, Di Ilio A. An experimental study on clinched joints realized with different dies. Thin-Walled Struct. 2014;85:71–80. doi: 10.1016/j.tws.2014.08.004

[8] Gay A, Roche J-M, Lapeyronnie P, et al. Non-destructive inspection of initial defects of PA6.6-GF50/aluminum self-piercing riveted joints and damage monitoring under mechanical static loading. Int J Damage Mech. 2017;26(8):1127–1146. doi: 10.1177/1056789516648370

[9] Haris A, Tay TE, Tan VBC. Experimental analysis of composite bolted joints using digital image correlation. J Mech Eng Sci. 2017;14(1):2443–2455. doi: 10.15282/jmes.11.1.2017.4.0225

[10] Jäckel M, Coppieters S, Vandermeiren N, et al. Process-oriented flow curve determination at mechanical joining. Procedia Manuf. 2020;47:368–374. doi: 10.1016/j.promfg.2020.04.289

[11] Zhang Y, Zhang X, Guo J, et al. Effects of local stiffness on the spot joints mechanical properties: comparative study between resistance spot welding and resistance spot clinching joints. J Manuf Processes. 2019;39:93–101. doi: 10.1016/j.jmapro.2019.02.018

[12] Zhang Y, Shan H, Li Y, et al. Joining aluminum alloy 5052 sheets via novel hybrid resistance spot clinching process. Mater & Des. 2017;118:36–43. doi: 10.1016/j.matdes.2017.01.017

[13] Philip RE, Andrushia AD, Nammalvar A, et al. A comparative study on crack detection in concrete walls using transfer learning techniques. J Compos Sci. 2023;7(4):169. doi: 10.3390/jcs7040169

[14] Roy K, Rezaeian H, Lakshmanan D, et al. Structural behaviour of cold-formed steel T-Stub connections with HRC and screws subjected to tension force. Eng Struct. 2023;283:115922. doi: 10.1016/j.engstruct.2023.115922

[15] Mathieson C, Roy K, Clifton GC, et al. Failure mechanism and bearing capacity of cold-formed steel trusses with HRC connectors. Eng Struct. 2019;201:109741. doi: 10.1016/j.engstruct.2019.109741

[16] Sutton MA, Orteu JJ, Schreier H. Image correlation for shape, motion and deformation measurements: basic concepts, theory and applications. New York (NY): Springer Science & Business Media; 2009.

[17] Górszczyk J, Malicki K, Zych TJM. Application of digital image correlation (DIC) method for road material testing. Materials. 2019;12(15):2349. doi: 10.3390/ma12152349

[18] JIS G 3141. (English): cold-reduced carbon steel sheet and strip. Japanese standards association, Tokyo, 107-8440 JAPAN. 2005.

[19] ISO 12996. Mechanical joining—destructive testing of joints—specimen dimensions and test procedure for tensile shear testing of single joints. Geneva, Switzerland: ISO; 2013.

[20] Mucha J, Boda L, Witkowski W. The energy consumption of the process of joining steel sheets with the use of clinching with and without an additional rivet, and analysis of sheet deformation and mechanical strength of joints. 2023, PREPRINT (Version 1) available at Research Square, July 13. doi: 10.21203/rs.3.rs-3166946/v1

[21] Ren X, Chen C, Peng H, et al. Investigation on mechanical behavior of clinched joints produced with dissimilar dies. Proc Inst Mech Eng Part B: J Eng Manufacture. 2023;237 (1–2):31–42. doi: 10.1177/09544054221092910

[22] Technical S. TECHNICAL DATA SHEET USA2012. 2023 [cited 2023 Jun 7]. Available from: http://www.silock.com.my/product.php?cid=4

[23] Eshtayeh M, Hijazi A, Hrairi M. Nondestructive evaluation of welded joints using digital image correlation. J Nondestruct Eval. 2015;34(4):1–12. doi: 10.1007/s10921-015-0310-z